

# Adeno-associated virus-mediated neuroglobin overexpression ameliorates the N-methyl-N-nitrosourea-induced retinal impairments: a novel therapeutic strategy against photoreceptor degeneration

Ye Tao,<sup>1,\*</sup> Zhen Yang,<sup>2,\*</sup>  
Wei Fang,<sup>2</sup> Zhao Ma,<sup>3</sup> Yi  
Fei Huang,<sup>1</sup> Zhengwei Li<sup>4</sup>

<sup>1</sup>Department of Ophthalmology, Key Lab of Ophthalmology and Visual Science, Chinese PLA General Hospital, Beijing, <sup>2</sup>Department of Neurosurgery, Institute for Functional Brain Disorders, Tangdu Hospital, Fourth Military Medical University, Xi'an, <sup>3</sup>Department of Neurosurgery, Central Hospital of Wuhan, Tongji Medical College, Huazhong University of Science and Technology, <sup>4</sup>Department of Neurosurgery, Zhongnan Hospital of Wuhan University, Wuhan, People's Republic of China

\*These authors contributed equally to this work

Correspondence: Yi Fei Huang  
Department of Ophthalmology, Chinese PLA General Hospital, 28 Fuxing Road, Haidian District, Beijing 100853, People's Republic of China  
Tel +86 10 6693 7943  
Fax +86 10 6828 6682  
Email huangyf301@163.com

Zhengwei Li  
Department of Neurosurgery, Zhongnan Hospital of Wuhan University, Wuhan 430071, People's Republic of China  
Tel +86 13 66 508 2290  
Fax +86 13 66 508 2581  
Email xiulilidr@163.com

**Abstract:** Retinal degeneration (RD) is a heterogeneous group of inherited dystrophies leading to blindness. The N-methyl-N-nitrosourea (MNU)-administered mouse is used as a pharmacologically induced RD animal model in various therapeutic investigations. The present study found the retinal neuroglobin (NGB) expression in the MNU-administered mice was significantly lower than in normal controls, suggesting NGB was correlated with RD. Subsequently, an adeno-associated virus (AAV)-2-mCMV-NGB vector was delivered into the subretinal space of the MNU-administered mice. The retinal NGB expression of the treated eye was upregulated significantly in both protein and mRNA levels. Further, we found NGB overexpression could alleviate visual impairments and morphological devastations in MNU-administered mice. NGB overexpression could rectify apoptotic abnormalities and ameliorate oxidative stress in MNU-administered mice, thereby promoting photoreceptor survival. The cone photoreceptors in MNU-administered mice were also sensitive to AAV-mediated NGB overexpression. Taken together, our findings suggest that manipulating NGB bioactivity via gene therapy may represent a novel therapeutic strategy against RD. Future elucidation of the exact role of NGB would advance our knowledge about the pathological mechanisms underlying RD.

**Keywords:** neuroglobin, retinal degeneration, photoreceptor

## Introduction

As a critical component of the central nerve system, the retina is responsible for the conversion of light stimulus into electrical spikes which are subsequently interpreted in the visual cortex as visual function.<sup>1,2</sup> Retinal degeneration (RD) is a heterogeneous group of inherited dystrophies characterized by the progressive apoptosis of retinal neurons and irreversible visual disturbance. Typically, an outcome of blindness occurs within several decades after the onset of RD.<sup>3</sup> In the past decades, there has been a constant increase in the discovery of a number of initiated gene mutations that cause RD. Given the tremendous genetic heterogeneity implied in RD, the kinetics of progression, the severity of visual impairments, and the secondary clinical signs are all considerably variable even in individuals from the same family. These complexities constitute a myriad of intrinsic obstacles against photoreceptor rescue and visual function restoration in patients with RD. Accordingly, animal models are desirable

for disclosing the underlying mechanisms and developing therapeutic tools against RD.<sup>4</sup> N-methyl-N-nitrosourea (MNU), as an alkylating carcinogen, is capable of mediating selective photoreceptor apoptosis in mammalian retinas, thereby generating a pharmacologically induced animal model of RD.<sup>5,6</sup> After a single systemic administration, MNU toxicity induces active signs of RD, such as decreased outer nuclear layer (ONL) thickness, impaired electroretinogram (ERG) response, and hyper-expressed apoptotic labeling. Generally, this degenerative process in mouse retina is accomplished within 7 days with the administered dose of 60 mg/kg. Therefore, the MNU-administered mouse serves as a pharmacologically induced RP model with rapidly progressive dynamics. Notably, oxidative stress is recognized as a critical initiator in MNU-induced RD.<sup>7,8</sup> Reactive oxygen species (ROS) resulting from protein alkylation can activate member proteins of the Bax/Bak family, disrupt mitochondrial membrane potential, enhance the permeability of transition pores, and promote cytochrome C release, which ultimately triggers the caspase-mediated apoptotic cascades. This pathological mechanism shares many common features with that occurring in the hereditary RP models. Therefore, the MNU-administered animal model has been used in several pathophysiologic and therapeutic investigations.<sup>9,10</sup>

Neuroglobin (NGB) is a member of globin superfamily that is selectively distributed in neural tissues.<sup>11</sup> NGB features an iron-containing central heme group and an-helical polypeptide which confers on it an oxygen-binding property. The highest NGB expression is found in the retina, especially those retinal layers with preferential vulnerability to oxidative stress.<sup>12</sup> NGB could facilitate oxygen metabolism in retinal neurons. At the subcellular level, NGB co-localizes with the mitochondria, which plays a key role in cellular homeostasis. These findings highlight the close correlation between NGB and mitochondrial function.<sup>13,14</sup> NGB would not only participate in oxygen storage or transportation, but also serve as an oxygen signaling sensor. NGB is very sensitive to fluctuations in oxygen level or inadequate blood supply. Endogenous NGB expression is upregulated in response to ischemia, hypoxia, oxidation, and toxicity.<sup>15–17</sup> Enhanced NGB expression might be considered an endogenous compensatory or protective mechanism, as evidenced by decrease in mitochondrial damage and lesser activation of apoptotic cascades. This notion is further reinforced by the fact that NGB overexpression via gene transactivators alleviates hypoxic/ischemic insults, oxidative impairments, and neurodegenerative disorders.<sup>18,19</sup> Conversely, NGB

deprivation via gene knockout induces deterioration in the outcomes of these pathological conditions.<sup>20</sup>

In the present study, we examined retinal NGB expressions in MNU-administered mice and found these were significantly lower than in normal controls. Subsequently, we delivered the adeno-associated virus (AAV)-2-Mcmv-NGB vector into the subretinal space of MNU-administered mice to enhance retinal NGB expressions. NGB overexpression alleviated effectively MNU-induced RD. Therefore, it could be concluded that NGB plays a critical role in retinal homeostasis and entails longer photoreceptor survival under oxidative stress. The NGB may serve as a promising therapeutic target against RD.

## Materials and methods

### Animals

The C57BL/6 mice (male, 8 weeks old) were purchased from Laboratory Animal Center of the General Hospital of PLA (Beijing, People's Republic of China), and housed in an air-conditioned animal facility (room temperature: 18°C–23°C, humidity: 40%–65%) on a 12-hour light/dark cycle. Care and maintenance of animals were carried out in compliance with the ARVO guidelines for the Use of Animals in Ophthalmic and Vision Research. All procedures with regard to the use and handling of the animals were approved by the Institutional Animal Care and Use Committee of the General Hospital of Chinese PLA. To induce photoreceptor degeneration, the mouse received an intraperitoneal injection of MNU (60 mg/kg; Sigma; St Louis, MO, USA) that was dissolved in physiologic saline containing 0.05% acetic acid. One eye of the MNU-administered mouse received a subretinal injection of AAV2/2-mCMV-NGB vectors 1 week prior to MNU administration. The other eye was left untreated with the vectors as a control.

### Construct of viral vectors and subretinal injections

The full-length NGB mRNA sequence (1,630 base pairs, including the mouse NGB open reading frame and associated 5'UTR and 3'UTR) was cloned under the transcriptional control of a cytomegalovirus (mCMV) promoter to generate the vector plasmid. Then, the vector DNA was packed into the AAV2/2 plasmid which would confer high transduction efficiency and faster onset of expression in photoreceptors. The final constructs were produced by the ENECHEM biological company's virus production core in Shanghai, People's Republic of China. The packaged viruses were concentrated and purified in phosphate-buffered saline (PBS)

with a titer of  $6.0 \times 10^{12}$  AAV2/2-NGB genome copies per mL. For treatment, 1  $\mu$ L of the vector suspension was injected into the subretinal space of mouse eye according to a previously described method.<sup>21</sup> On reaching the subretinal cavity, the therapeutic agents would exert beneficial effects on neighboring photoreceptors. The whole procedure of subretinal injection is very elaborate and should be carried out under the direct microscopic visualization. Briefly, the anesthetized mice were moved to an animal operating table under a dissecting microscope. A 30  $\frac{1}{2}$ -gauge disposable beveled needle was used to make an incision near the corneal limbus. The syringe needle of a Hamilton micro injector (Hamilton Company, Reno, NV, USA) was inserted into the anterior chamber through the corneal perforation. The plunger of the Hamilton syringe was slowly pushed to deliver the reagent to the targeted space. The needle should not be pushed beyond the retinal inner surface. If the inserting depth is not properly handled, the operation would cause significant retinal damage associated with fundal hemorrhage. Thereafter, the needle was carefully withdrawn and neomycin/polymyxin B ophthalmic ointment (Xing Qi, Shenyang, People's Republic of China) was applied to the injected eyes to avoid infection. The injected eyes were examined once a day to verify whether any complications (eg, cataracts, retinal hemorrhage and infection) occurred after subretinal injection. These injected mice with complications were excluded from further evaluation.

## ERG recording

One week after MNU administration, the dark-adapted animals were anesthetized by an intraperitoneal injection of ketamine (80 mg/kg) and chlorpromazine (15 mg/kg, Jilin Shengda Animal Pharmaceutical Co., Ltd, People's Republic of China). Their pupils were dilated with 1% atropine and 2.5% phenylephrine hydrochloride (Xing Qi, Shenyang, People's Republic of China). Subsequently, they were transferred to the recording platform under dim red light. The cornea was anesthetized with a drop of 0.5% proxymetacaine. The RETIport system (Roland Consult, Germany) with custom-made chloride silver electrodes was used in the ERG recording. A loop electrode was placed over the cornea to serve as the active electrode. Needle reference and ground electrodes were respectively inserted into the cheek and tail. A brief white flash ( $3.0 \text{ cd} \cdot \text{s/m}^2$ ) was delivered from a Ganzfeld integrating sphere to stimulate the response. The band-pass (1–300 Hz) was used to amplify the recorded signals. The line noise was wiped off by a 50-Hz notch filter. We collected and averaged 60 photopic and 10 scotopic responses for waves analysis.

## SD-OCT examination

After ERG recordings, the animals were transferred to the recording plane of the SD-OCT system (Biophtigen, Durham, NC) when they were anesthetized. Their pupils were dilated with 1% atropine and 2.5% phenylephrine hydrochloride (Xing Qi, Shenyang, People's Republic of China). A corresponding box was centered on the optic nerve head (ONH) with eight measurement points separated by 3 mm from each other. The SD-OCT cross-sectional images were analyzed with the InVivoVue<sup>TM</sup> DIVER 2.4 software (Biophtigen, Inc, NC, USA). The neural retinal thickness for examined eyes was compared at each point by measuring the distance from the vitreous face of the RGCs layer to the apical face of the RPE layer. OCT images were acquired after noise reduction of the average.

## Optokinetic testing

A week after MNU administration, the light-adapted visual acuity and contrast sensitivity of mice were measured using a two-alternative forced-choice paradigm as described previously.<sup>22</sup> Briefly, stepwise functions for correct responses in both the clockwise and counterclockwise direction were used to determine the response thresholds. The initial stimulus in visual acuity measurements was set as a 0.200 cyc/deg sinusoidal pattern with a fixed 100% contrast. The initial pattern in contrast sensitivity measurements was set as 100% contrast, with a fixed spatial frequency of 0.128 cyc/deg. All patterns were presented at a speed of 12 degrees/s with a mean luminance of 70  $\text{cd/m}^2$ . Visual acuities and contrast sensitivities of each mouse were measured four times over a period of 24 hours.

## Histology assessment and immunohistochemistry

One week after MNU administration, the animals were sacrificed and their eyecups were enucleated. The eye cups were immersed in a fixative solution 4% paraformaldehyde (Dulbecco's PBS; Mediatech, Inc., Herndon, VA) for 24 hours. They were rinsed with phosphate buffer (PB), dehydrated in a graded ethanol series, and embedded in paraffin wax. Five sections of 5- $\mu$ m thickness were cut vertically through the ONH of each eye. The sections were stained with hematoxylin and eosin (HE) and were evaluated by light microscopy. With the aid of Image-Pro Plus software (Media Cybernetics, Silver Spring, MD), the adjacent thickness of the ONL was measured along the vertically superior–inferior axis at 250- $\mu$ m intervals. The mean ONL thickness of each mouse was averaged from five sections. Then

sections were rinsed in 0.01 M PBS, permeabilized in 0.3% Triton X-100, and blocked in 3% BSA for 1 hour at room temperature. The peanut agglutinin conjugated to a Alexa Fluor 488 (1:200, L21409, Invitrogen, USA), polyclonal S-cone opsin, and M-cone opsin antibodies (1:400, Millipore, MA, USA) were diluted in 0.1% Triton X-100 and 1% BSA in PBS, and incubated with sections overnight at 4°C. The sections were extensively washed with PBS, and then incubated in Cy3-conjugated anti-rabbit IgG (1:400, 711-165-152, Jackson ImmunoResearch Laboratories, USA). The sections were rapidly rinsed five times with 0.01 M PBS, and then coverslipped with anti-fade Vectashield mounting medium (Vector Laboratories, Burlingame, CA, USA) for photographing.

### Quantification of superoxide dismutase (SOD) activity and malondialdehyde (MDA) content

Three days post MNU administration, the animals were sacrificed and their eyecups were enucleated. The retinal tissue was added into the PBS containing 0.5% Triton X-100 (pH 7.4) and then homogenized in ice-cold Tris-HCl medium using grinders. The retinal tissue was centrifuged at 500× g for 5 minutes at 4°C. The tissue suspension was assayed for protein content to normalize enzymatic activity and MDA content, a presumptive marker of oxidant-mediated lipid peroxidation. The SOD activity was examined with the SOD Assay Kit-WST (Jiancheng Biotech Ltd., Nanjing, People's Republic of China). A spectrophotometer with ultra-microcuvettes was used to measure absorbance values. The content of MDA was assessed using a total bile acids colorimetric assay according to manufacturer instructions (Jiancheng Biotech Ltd., Nanjing, People's Republic of China).

### Western blot analysis

A week after MNU administration, the retinas were cut into pieces and homogenized in buffer containing 0.23 mmol sucrose, 2 mmol EDTA, 5 mmol Tris-HCl (pH 7.5), and 0.1 mmol phenylmethylsulfonyl fluoride. After centrifugation, aliquot extracts containing equal amounts of protein (20 µg) were electrophoresed, transferred, and probed with a rabbit anti-rat polyclonal anti-mouse antibody (1:500, Santa Cruz Biotechnology, Inc., Santa Cruz, CA, USA). The membrane was washed thoroughly and then incubated with HRP-conjugated goat anti-rabbit IgG antibody (1:1,000, Santa Cruz Biotechnology, CA). Bands were visualized using an enhanced chemiluminescence detection system (Super Signal ECL kit; West Pico; Pierce, Rockford, IL, USA).

### Quantitative reverse transcription-polymerase chain reaction (qRT-PCR)

Three days post MNU administration, the total RNA was extracted from pooled retinal patches with a commercial reagent (Trizol, Gibco Inc., Grand Island, NY, USA), followed by cDNA synthesis using the µMACS™ DNA Synthesis kit (Miltenyi Biotech GmbH, Bergisch-Gladbach, Germany). GAPDH was used as an internal standard of mRNA expression. Reactions were carried out in a real-time CFX96 Touch PCR detection system (Bio-Rad Laboratories, Reinach, Switzerland). The amplification program consisted of polymerase activation at 95°C for 5 minutes and 50 cycles of denaturation at 95°C for 1 minute, followed by annealing and extension at 59°C for 30 seconds.

The primers used in qRT-PCR were: Bax:5'-AGCTCTGAACAGATCATGAAGACA-3' (forward) and 5'-CTCCATGTTGTTGTCCAGTTCATC-3' (reverse); Bcl-2:5'-GGACAACATCGCTCTGTGGATGA-3' (forward) and 5'-CAGAGACAGCCAGGAGAAATCAA-3' (reverse); Caspase-3:5'-TGTCGATGCAGCTAACCC-3' (forward) and 5'-GGCCTCCACTGGTATCTTCTG-3' (reverse); Chop:5'-CTGCCTTTTACCTTGGAGAC-3' (forward) and 5'-CGTTTCCTGGGGATGAGATA-3' (reverse); Caspase-12:5'-CTGACCCAGATGCCCCACTAT-3' (forward) and 5'-CCTGGGATCTTGGAATTTTCT-3' (reverse); Atg-5:5'-ACTGTCCATCTGCAGCCAC-3' (forward) and 5'-GCCATCAATCGGAAACTCAT-3' (reverse); Calpian-2:5'-CCCCAGTTCATTATTGGAGG3' (forward) and 5'-GCCAGGATTTCTCATTC AA-3' (reverse); Caspase-9:5'-GCCTCATCATCAACAACG-3' (forward) and 5'-CTGGTATGGGACAGCATCT-3' (reverse); NGB:5'-TACAATGGCCGCCAGTTCT3' (forward) and 5'-TGGTCACTGCAGCATCAATCA-3' (reverse). The relative expression levels were normalized and quantified to obtain the  $\Delta\Delta^{CT}$  values (DATA assist Software v2.2, Applied Biosystems).

### Statistical analysis

The statistical difference between the animal groups was processed using ANOVA followed by Bonferroni's post hoc analysis.  $P < 0.05$  was considered significant. The values are presented as mean  $\pm$  standard deviation (SD).

## Results

### NGB expressions in the retinas of MNU-administered mice

No death occurred during the whole process of MNU administration. The Western blot study suggested the retinal



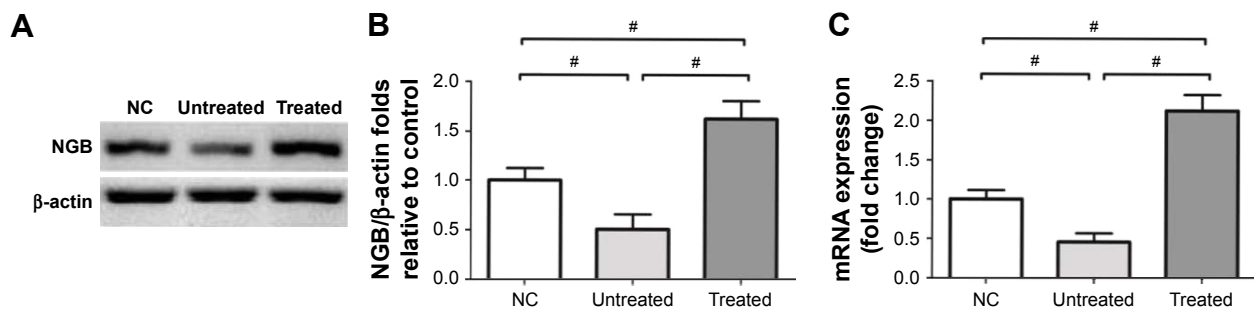


**Figure 1** (A) The Western blot study suggested that retinal NGB expression in untreated eyes was significantly lower than in normal controls. (B) The retinal NGB level in the treated eyes was significantly higher than in normal controls. The retinal NGB level in the treated eyes was significantly higher than in untreated eyes, suggesting the AAV vector mediated pronounced NGB overexpression in the treated eyes. (C) The mRNA level of NGB in untreated eyes was significantly lower than that in normal controls. However, the mRNA level of NGB in the treated eyes was significantly higher than in normal controls. All values are presented as mean  $\pm$  SD; \* $P < 0.01$  for differences compared between eye groups.

**Abbreviations:** NGB, neuroglobin; NC, normal control; AAV, adeno-associated virus.

NGB expression in the untreated eyes was significantly lower than the normal controls ( $P < 0.01$ ;  $n = 10$ ; Figure 1A). On the contrary, the retinal NGB level in the treated eyes was significantly higher than in normal controls ( $P < 0.01$ ;  $n = 10$ ). The retinal NGB level in the treated eyes was also significantly higher than in untreated eyes ( $P < 0.01$ ;  $n = 10$ ), suggesting the AAV vector could mediate NGB overexpression in mouse retina. Subsequently, the qRT-PCR study was conducted to quantify mRNA levels of NGB. The mRNA level of NGB in the untreated eyes was significantly lower than in normal controls ( $P < 0.01$ ;  $n = 10$ ; Figure 1B). However, the mRNA level of NGB in the treated eyes was significantly higher than in normal controls ( $P < 0.01$ ;  $n = 10$ ).

### NGB overexpression ameliorated MNU-induced visual functional impairments

Experimental animals were subjected to optokinetic behavioral tests. The untreated eyes responded poorly to rotating sinusoidal gratings. Both the visual acuity and contrast sensitivity of the untreated eyes were significantly lower than in normal controls ( $P < 0.01$ ;  $n = 10$ ; Figure 2A). On the other hand, the performances of the treated eyes were much better than of untreated eyes. Both visual acuity and contrast sensitivity of the treated eyes were significantly higher than the untreated eyes ( $P < 0.01$ ;  $n = 10$ ), suggesting the AAV2-mediated NGB overexpression could improve the optokinetic function of MNU-administered eyes. Meanwhile, the visual acuity and the contrast sensitivity of the treated eyes were relatively lower than in normal controls (visual acuity:  $P < 0.05$ ,  $n = 10$ ; contrast sensitivity:  $P < 0.01$ ,  $n = 10$ ). Subsequently, the experimental animals were subjected to ERG examination. The representative waveforms of ERG responses are shown in Figure 2B. MNU induced severe impairments in untreated eyes, as no reliable ERG waveform

was detected in these eyes. The photopic and scotopic b-wave amplitudes of the untreated eyes were significantly smaller than those of normal controls ( $P < 0.01$ ;  $n = 10$ ; Figure 2C). Notably, the treated eyes exhibited less impaired ERGs. Both the photopic and scotopic b-wave amplitudes of treated eyes were significantly larger than those in untreated eyes ( $P < 0.01$ ;  $n = 10$ ), suggesting AAV2-mediated NGB overexpression could ameliorate visual functional impairments.

### NGB overexpression alleviated photoreceptor degeneration in MNU-administered mice

Experimental animals were subjected to SD-OCT examination and their retinal thicknesses were quantified in vivo (Figure 3A). The retinal organization of the untreated eyes was severely disrupted by MNU administration. The retinal thickness of the untreated eyes was substantially smaller than in normal controls ( $P < 0.01$ ;  $n = 10$ ). The retinal thickness of the treated eyes was also significantly smaller than in normal controls ( $P < 0.01$ ;  $n = 10$ ). However, the retinal thickness of the treated eyes was significantly larger than the untreated eyes ( $P < 0.01$ ;  $n = 10$ ), suggesting that the MNU induced morphological injury could be partly alleviated by NGB overexpression. Subsequently, the ONL thickness was measured to quantify the viability of photoreceptors (Figure 3B). The ONL of the untreated eyes disappeared after MNU administration. Conversely, a large proportion of ONL was retained in the treated eyes. The average ONL thickness of the treated eyes was significantly smaller than that in normal controls ( $P < 0.01$ ;  $n = 10$ ). However, it was significantly larger than in untreated eyes ( $P < 0.01$ ;  $n = 10$ ). Collectively, these findings suggest that AAV2-mediated NGB overexpression could alleviate RD and enhance photoreceptor survival in MNU-administered mice.

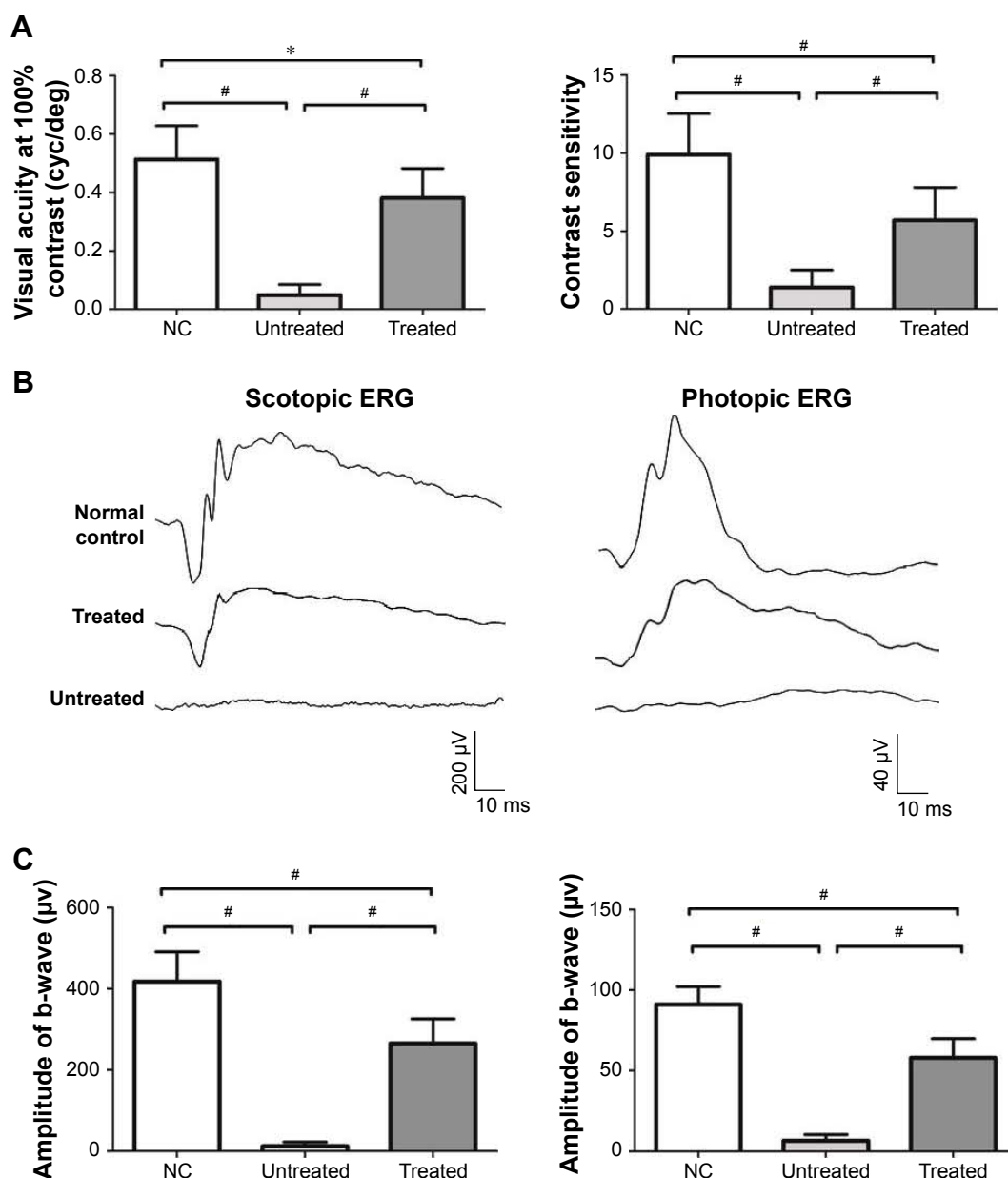


**Figure 2** (A) The visual acuity and contrast sensitivity of untreated eyes were significantly lower than in normal controls, whereas visual acuity and contrast sensitivity of the treated eyes were both significantly higher than in the untreated eyes. Meanwhile, visual acuity and the contrast sensitivity of the treated eyes were significantly lower than in normal controls. (B) Representative ERG waveforms of different eye groups. (C) The photopic and scotopic b-wave amplitudes of untreated eyes were significantly smaller than in normal controls. Both photopic and scotopic b-wave amplitudes of treated eyes were significantly larger than those of the untreated eyes, suggesting NGB overexpression could ameliorate MNU-induced visual functional impairments. All values are presented as mean  $\pm$  SD; \* $P < 0.05$  for differences compared between eye groups; # $P < 0.01$  for differences compared between eye groups.

**Abbreviations:** ERG, electroretinogram; MNU, N-methyl-N-nitrosourea; NGB, neuroglobin; NC, normal control.

As the rods account for the majority of photoreceptor populations in murine retina (~97%), the ONL should be considered as an indicator of the rod viability.<sup>23</sup> Whether the minority cones (~3%) were rescued by NGB overexpression could not be deduced from HE-stained sections. Therefore, we conducted immunostaining experiments to verify the viability of cones in retinas (Figure 4A). Typical PNA staining was detected in the ONL of normal controls. However, no PNA staining was detected in retinas of

untreated eyes, suggesting the cones were eliminated absolutely by MNU toxicity. In contrast, a substantial portion of PNA staining was detected in retinas of the treated eyes, suggesting that the cone photoreceptors were sensitive to NGB treatment. In greater detail, we analyzed immunostaining with M- and S-opsin antibodies. Both M- and S-opsin staining was detected throughout the retina of the treated eyes, although with a relatively decayed intensity than in normal controls.

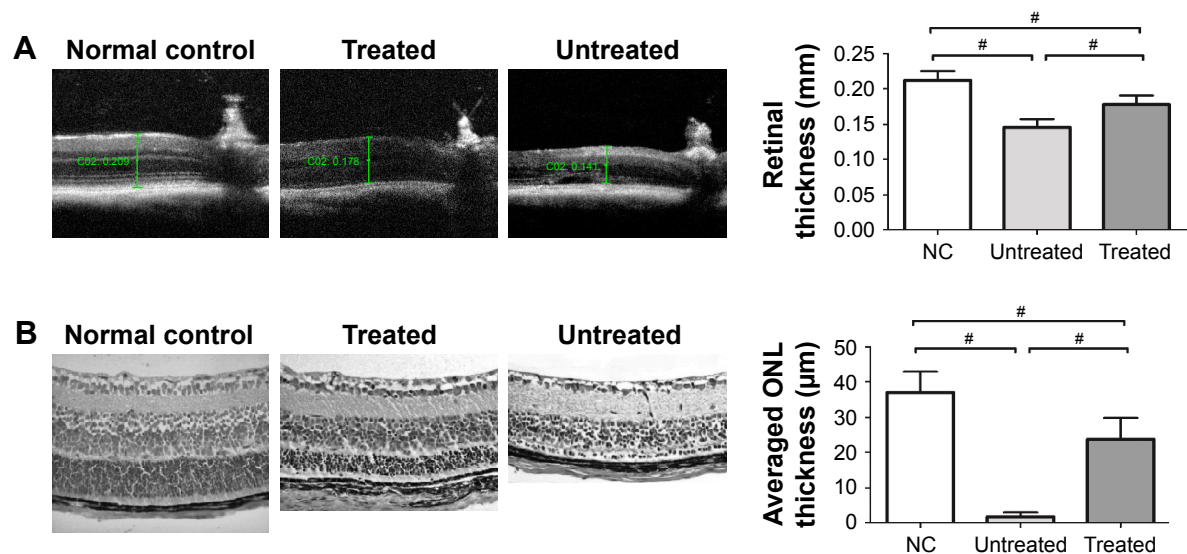


**Figure 3 (A)** Experimental animals were subjected to SD-OCT examination and their retinal thicknesses were quantified in vivo. Retinal thickness of the treated eyes was significantly smaller than that of normal controls. However, the retinal thickness of the treated eyes was significantly larger than that of untreated eyes. **(B)** The ONL of the untreated eyes disappeared after MNU administration. Conversely, a large proportion of ONL was retained in the retinas of treated eyes. The average ONL thickness of the treated eyes was significantly smaller than that of normal controls. The average ONL thickness of the treated eyes was significantly larger than that of the untreated eyes. All values are presented as mean  $\pm$  SD;  $^{\#}P < 0.01$  for differences compared between eye groups.

**Abbreviations:** MNU, N-methyl-N-nitrosourea; NC, normal control; ONL, outer nuclear layer; SD-OCT, spectral domain-optical coherence tomography.

## Mechanisms underlying NGB-mediated protection

MDA is a reactive electrophile species that causes toxic impairments to polyunsaturated fatty acids. MDA reflects the level of lipid peroxidation caused by free radicals and is

considered as a presumptive marker of oxidation. The retinal MDA concentration in the treated eyes was significantly lower than in untreated eyes ( $P < 0.01$ ;  $n = 10$ , Figure 4B). The retinal SOD level in treated eyes was significantly higher than in untreated eyes ( $P < 0.01$ ;  $n = 10$ , Figure 4B), suggesting that

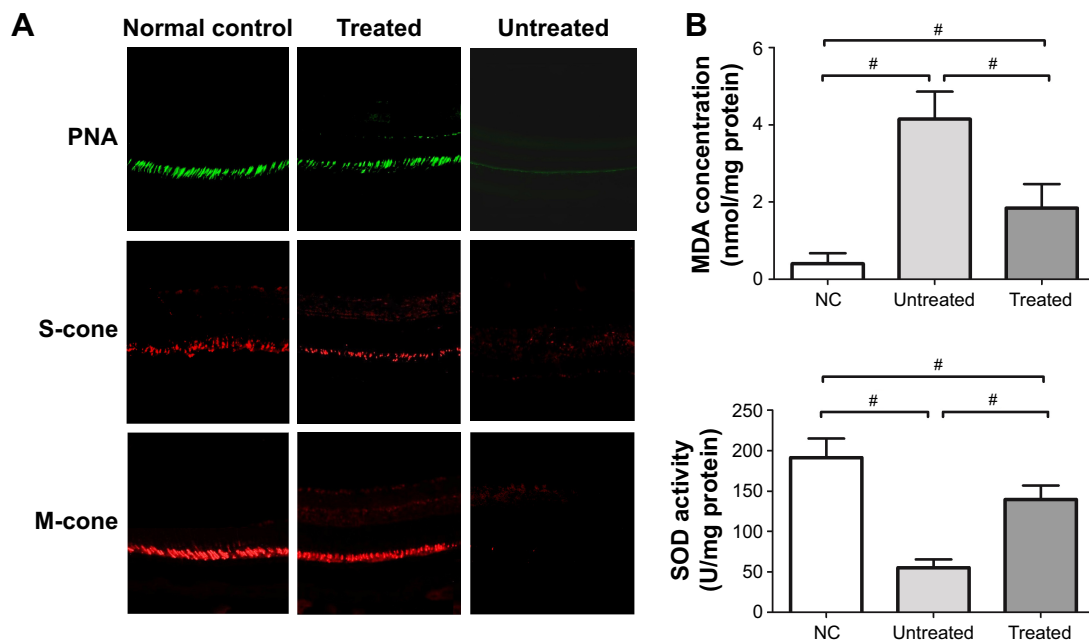


**Figure 4 (A)** The typical PNA staining was detected in the ONL of normal controls. However, no PNA staining was found in the retinas of untreated eyes. A substantial portion of PNA staining was detected in the retinas of the treated eyes. Both M- and S-opsin staining was detected throughout the retina of the treated eyes, although with a relatively decayed manner as compared with normal controls. **(B)** Retinal MDA concentration of the treated eyes was significantly lower than those of untreated eyes. The retinal SOD level in treated eyes was significantly higher than in untreated eyes, suggesting that the oxidative stress in the MNU-administered eyes was alleviated by NGB treatment. All values are presented as mean  $\pm$  SD;  $^{\#}P < 0.01$  for differences compared between eye groups.

**Abbreviations:** MDA, malondialdehyde; MNU, N-methyl-N-nitrosourea; NGB, neuroglobin; NC, normal control; ONL, outer nuclear layer; PNA, peanut agglutinin; SOD, superoxide dismutase.

oxidative stress in MNU-administered mice was alleviated by NGB overexpression. Subsequently, we conducted qRT-PCR to analyze the mechanisms underlying NGB-induced protection. Retinal mRNA levels of bax, calpain-2, and caspase-3 in the treated eyes were significantly lower than in untreated eyes ( $P < 0.01$ ;  $n = 10$ ; Figure 5). On the other hand, the mRNA level of Bcl-2 in the treated eyes was significantly higher than in untreated eyes ( $P < 0.01$ ;  $n = 10$ ). In the untreated eyes, the mRNA levels of several ER stress sensors including C/EBP-homologous protein (CHOP), caspase-9, and caspase-12, were significantly higher than in normal controls ( $P < 0.01$ ;  $n = 10$ ). Expression levels of these ER stress sensors in the untreated eyes were not significantly different from those in treated eyes ( $P < 0.05$ ;  $n = 10$ ). Additionally, we examined the expression level of autophagy-related protein 5 (Atg-5), which is a well-characterized maker of autophagy. The mRNA level of Atg5 in the untreated eyes was significantly lower than in normal controls ( $P < 0.05$ ;  $n = 10$ ). However, the mRNA level of Atg5 in treated eyes was significantly higher than in untreated eyes ( $P < 0.05$ ;  $n = 10$ ), suggesting NGB treatment could partially restore basal autophagy in MNU-administered mice.

## Discussion

As a member of the globin superfamily, NGB is initially recognized as an oxygen transporter in neural tissues. Accumulating evidences suggest the NGB serves as an endogenous neuroprotectant against hypoxic/ischemic insults.<sup>24</sup>

NGB is present at a 100-fold greater concentration in the retina than in the brain, implying that the retina may be the most important site of NGB function.<sup>13,25</sup> However, evidence on the etiological contribution of NGB is just emerging in retinal diseases. Therefore, we examined the retinal NGB expression in MNU-administered mice. NGB expression decreased significantly during photoreceptor degeneration. For the first time, we demonstrate NGB is correlated with RD, highlighting that NGB overexpression via gene strategies may be therapeutically effective. Photoreceptors are the most metabolically active neurons in retina. Their cellular architecture is exquisitely designed to host a high concentration of molecules that participate in light capture, phototransduction, electrical signaling, and network activities.<sup>26</sup> Generally, these complex functions entail enormous metabolic demands and oxygen consumption. Given the critical role of NGB in oxygen metabolism, it is not surprising that NGB depletion is involved in photoreceptor degeneration.

Advances in molecular tools would facilitate the identification of the genetic defects underlying RD, and lead to the successful implementation of gene therapy.<sup>27</sup> AAV vectors have many attractive advantages, such as their lack of pathogenesis, low toxicity, early onset, and long-term gene transduction. On the other hand, the subretinal cavity has a relatively high degree of immune privilege and is recognized as an ideal space for drug delivery.<sup>21,28</sup> Therefore, these features are utilized to build our therapeutic trials. The AAV2-mCMV-NGB vector is constructed and injected

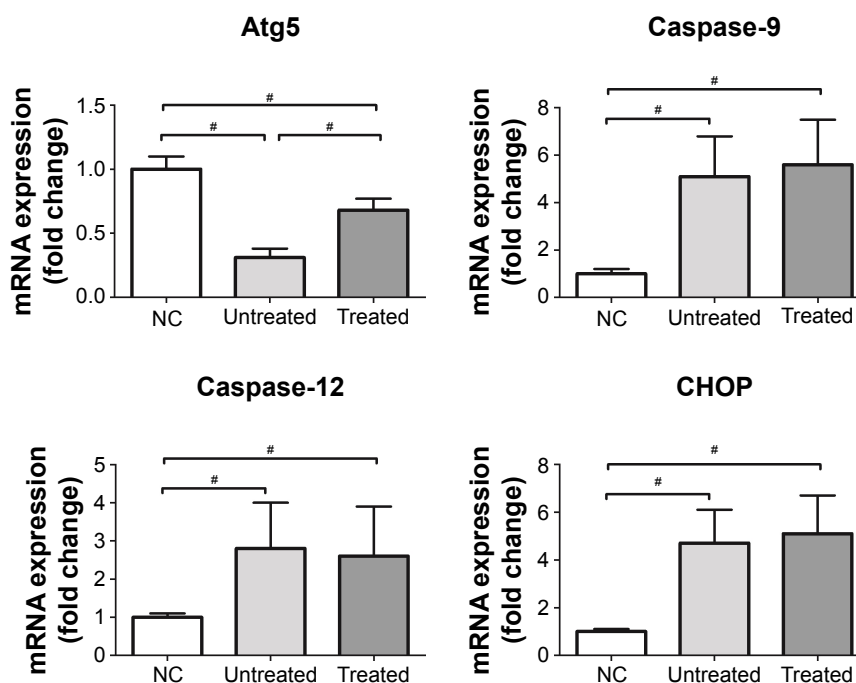
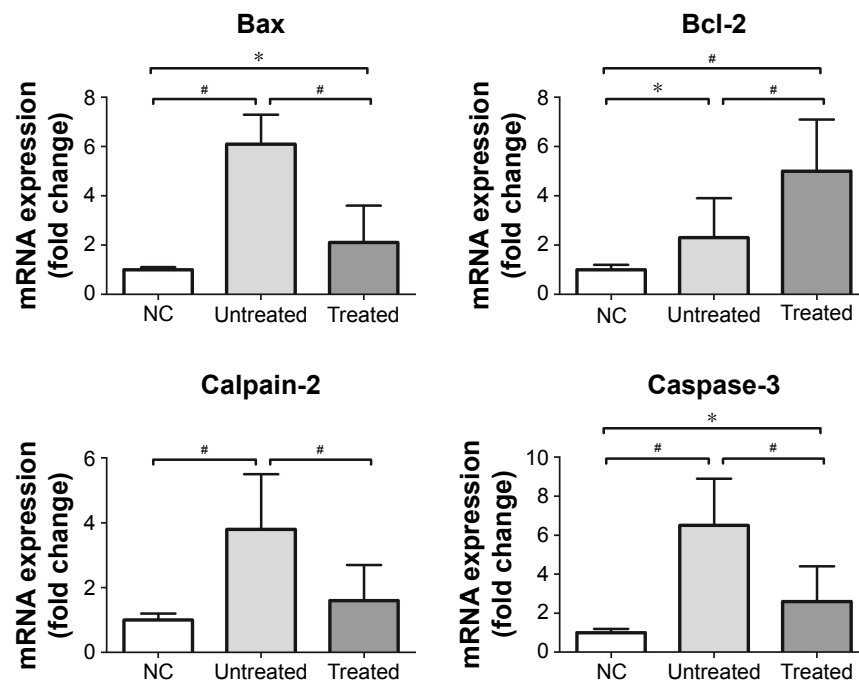


Figure 5 (Continued)





**Figure 5** The retinal mRNA levels of bax, calpain-2, and caspase-3 in the treated eyes were significantly lower than in untreated eyes. On the other hand, the mRNA level of bcl-2 in the treated eyes was significantly higher than in untreated eyes. In untreated eyes, mRNA levels of CHOP, caspase-9, and caspase-12 were significantly higher than in normal controls. Expression levels of these ER stress sensors in the untreated eyes were not significantly different from those in the treated eyes. The mRNA level of Atg5 in untreated eyes was significantly lower than in normal controls. However, the mRNA level of Atg5 in treated eyes was significantly higher than in untreated eyes. All values are presented as mean  $\pm$  SD; \* $P$ <0.05 for differences compared between eye groups; # $P$ <0.01 for differences compared between eye groups.

**Abbreviations:** CHOP, C/EBP-homologous protein; NC, normal control.

into the subretinal space of MNU-administered mice. After subretinal delivery, the AAV serotype 2 demonstrates potent transduction efficiency of therapeutic genes in the treated eyes. Moreover, the NGB expression level inversely correlates with the severity of RD in MNU-administered mouse. The treated eye responds better in the optokinetic behavioral test and ERG examination than the contralateral untreated eye. In accordance with improved visual function, the retinal architecture of the treated eye is much more intact than in the untreated eye. Collectively, these findings suggest that AAV2-mediated NGB overexpression could alleviate RD in MNU-administered mice. In greater detail, the therapeutic effects of NGB gene therapy on cone photoreceptors are validated by immunohistochemical studies. The cone photoreceptors were also rescued by NGB overexpression. NGB-mediated beneficial effects on cones are especially encouraging. As long as the cone photoreceptors are rescued, patients with RD might function well in well-lit environments and carry on relatively normal lives despite rod loss.<sup>29</sup> Further clinical studies are warranted to prove the effectiveness of NGB overexpression in the daily vision of patients with RD. Admittedly, some limitations are implicated in the MNU-induced RD model, and MNU-induced RD is rapidly progressing. However, RD is a relatively chronic retinopathy in human patients. Moreover, the observation that cones are

also killed by MNU toxicity does not correspond to cone degeneration in patients with RP, because the demise of this cone population occurs in a secondary wave of rod death. Therefore, although the outcome of the MNU administration partially resembles RD (ie, widespread rod death), the mechanistic underpinning and kinetics are very different.

The retina is one of the highest oxygen-consuming tissues in which the oxidative metabolism is finely modulated. When the balance between oxygen demand and supply is disturbed, the retina would be confronted with excessive ROS, which are detrimental to photoreceptors.<sup>30</sup> Accumulating evidences suggest that the oxidative stress is closely correlated with photoreceptor degeneration. Sustained bursts of intracellular ROS precede the disruption of mitochondrial transmembrane potential, nuclear condensation, DNA nicking, and cell shrinkage, all of which are hallmarks of photoreceptor apoptosis.<sup>31</sup> Herein, the enhanced NGB expression could endow the retina with abilities to combat with oxidative stress and apoptosis. In the treated retinas, the SOD activity increases while the MDA concentration decreases, suggesting the NGB could bolster the endogenous antioxidant enzymes and attenuate lipid oxidation.<sup>32,33</sup>

The mechanism underlying MNU-induced photoreceptor death is the principal alkylation of DNA, dependent on the action of alkyladenine DNA glycosylase (Aag); Aag would generate abasic sites that can be further processed by the base

excision repair machinery.<sup>34</sup> The MNU could induce 7MeG and 3MeA DNA lesions, both of which are Aag substrates, and photoreceptors would eventually turn into apoptosis when the repair process can no longer operate efficiently enough. The photoreceptor apoptosis is mainly mediated by conventional effectors. Herein, the mRNA levels of Bax and caspase-3, two mediators of the conventional apoptosis, are downregulated in the treated eyes. Meanwhile, the mRNA level of bcl-2, an anti-apoptotic factor is upregulated in the treated eyes. These findings suggest that NGB can rectify the changes in conventional apoptotic cascades to enhance photoreceptor survival. Moreover, it has been found that the alternative apoptotic pathways, including endoplasmic reticulum (ER) stress and calpain activation, are also involved in MNU-induced RD.<sup>35,36</sup> Cellular stress conditions, such as the perturbed calcium homeostasis and the accumulation of unfolded proteins, could activate ER stress in photoreceptors. In the present study, the mRNA levels of ER stress sensors, including CHOP, caspase-9, and caspase-12, in the untreated eye are significantly higher than those in normal controls. However, the mRNA levels of CHOP, caspase-9, and caspase-12 in the untreated eyes are not significantly different from those in the treated eyes. These findings suggest NGB overexpression would not affect the ER stress-mediated-apoptosis in the MNU-administered mouse. Additionally, basal autophagy functions as an essential survival mechanism by producing energy from the breakdown of deleterious cytoplasmic components. A pioneering study suggests basal autophagy in the photoreceptor is suppressed by calpain activation after MNU administration, highlighting autophagy would be involved in MNU-induced photoreceptor degeneration.<sup>37</sup> Atg-5 is required for the formation of autophagosomes and is considered a well-characterized maker of autophagy.<sup>38</sup> Herein, the mRNA level of Atg5 in the treated eyes was significantly higher than in untreated eyes, suggesting NGB treatment could partially restore the basal autophagy in MNU-administered mice.

Massive  $\text{Ca}^{2+}$  influx into the photoreceptors can trigger off calpain activation, apoptosis-inducing factor (AIF) induction, and eventually photoreceptor death.<sup>39,40</sup> To corroborate this notion, calcium channel blockers and calpain inhibitors have been utilized to counteract RD.<sup>41</sup> NGB reduces the calcium level in the ischemic retinas via the inositol trisphosphate (PI3) signal pathway.<sup>42</sup> NGB is also reported to couple with the membrane-bound G-protein coupled receptor (GPCR) to suppress elevated calcium levels.<sup>43</sup> Herein, NGB overexpression is associated with decreased mRNA level of calpain-2, a calcium-dependent cysteine protease. Taken

together, these findings suggest that NGB can function as a calpain inhibitor to alleviate RD.

## Conclusion

MNU administration reduces NGB expression in mouse retina, suggesting NGB is involved in RD. The AAV2 mediated NGB overexpression could rectify apoptotic abnormalities, alleviate oxidative stress, and thereby promote photoreceptor survival in MNU-administered mice. The exact mechanisms of RD in several retinopathies are not thoroughly understood. Currently, there is no satisfactory treatment to arrest RD in retinopathies such as retinitis pigmentosa, age-related macular degeneration, and achromatopsia. Therefore, our findings may shed light on the development of a promising therapeutic strategy against these diseases.

## Acknowledgments

This study was supported by grants from the National Key Basic Research Program of China (973 Program: 2013CB967001), National Natural Science Foundation of China (81600767, 81770887, and 81501063), the National key research and development plan of China (2017YFA0103204), and the Special Grant of Chinese Postdoctoral Science Foundation (2017T1000807).

## Disclosure

The authors report no conflicts of interest in this work.

## References

1. Moskowitz A, Hansen RM, Fulton AB. Retinal, visual, and refractive development in retinopathy of prematurity. *Eye Brain*. 2016;8: 103–111.
2. El-Shazly AAE, Farweez YA, Hamdi MM, El-Sherbiny NE. Pattern visual evoked potential, pattern electroretinogram, and retinal nerve fiber layer thickness in patients with migraine during and after aura. *Curr Eye Res*. 2017;42(9):1327–1332.
3. Strong S, Liew G, Michaelides M. Retinitis pigmentosa-associated cystoid macular oedema: pathogenesis and avenues of intervention. *Br J Ophthalmol*. 2017;101(1):31–37.
4. Geneva II. Photobiomodulation for the treatment of retinal diseases: a review. *Int J Ophthalmol*. 2016;9(1):145–152.
5. Tsubura A, Lai YC, Miki H, et al. Review: Animal models of N-Methyl-N-nitrosourea-induced mammary cancer and retinal degeneration with special emphasis on therapeutic trials. *In Vivo*. 2011;25(1):11–22.
6. Rösch S, Werner C, Müller F, Walter P. Photoreceptor degeneration by intravitreal injection of N-methyl-N-nitrosourea (MNU) in rabbits: a pilot study. *Graefes Arch Clin Exp Ophthalmol*. 2017;255(2): 317–331.
7. Tsuruma K, Yamauchi M, Inokuchi Y, Sugitani S, Shimazawa M, Hara H. Role of oxidative stress in retinal photoreceptor cell death in N-methyl-N-nitrosourea-treated mice. *J Pharmacol Sci*. 2012;118(3):351–362.
8. Hisano S, Koriyama Y, Ogai K, Sugitani K, Kato S. Nitric oxide synthase activation as a trigger of N-methyl-N-nitrosourea-induced photoreceptor cell death. *Adv Exp Med Biol*. 2016;854:379–384.

9. Tsubura A, Yoshizawa K, Kuwata M, Uehara N. Animal models for retinitis pigmentosa induced by MNU; disease progression, mechanisms and therapeutic trials. *Histol Histopathol*. 2010;25(7):933–944.
10. Emoto Y, Yoshizawa K, Uehara N, et al. Curcumin suppresses N-methyl-N-nitrosourea-induced photoreceptor apoptosis in Sprague-Dawley rats. *In Vivo*. 2013;27(5):583–590.
11. Burmester T, Weich B, Reinhardt S, Hankeln T. A vertebrate globin expressed in the brain. *Nature*. 2000;407(6803):520–523.
12. Hundahl CA, Fahrenkrug J, Luuk H, Hay-Schmidt A, Hannibal J. Restricted expression of Neuroglobin in the mouse retina and colocalization with Melanopsin and Tyrosine Hydroxylase. *Biochem Biophys Res Commun*. 2012;425(1):100–106.
13. Brittain T, Skommer J, Raychaudhuri S, Birch N. An antiapoptotic neuroprotective role for neuroglobin. *Int J Mol Sci*. 2010;11(6):2306–2321.
14. Brittain T, Skommer J. Does a redox cycle provide a mechanism for setting the capacity of neuroglobin to protect cells from apoptosis? *IUBMB Life*. 2012;64(5):419–422.
15. Yu Z, Liu N, Liu J, Yang K, Wang X. Neuroglobin, a novel target for endogenous neuroprotection against stroke and neurodegenerative disorders. *Int J Mol Sci*. 2012;13(6):6995–7014.
16. Liu A, Brittain T. A futile redox cycle involving neuroglobin observed at physiological temperature. *Int J Mol Sci*. 2015;16(8):20082–20094.
17. Wakasugi K, Nakano T, Kitatsuji C, Morishima I. Human neuroglobin interacts with flotillin-1, a lipid raft microdomain-associated protein. *Biochem Biophys Res Commun*. 2004;318(2):453–460.
18. Antao ST, Duong TT, Aran R, Witting PK. Neuroglobin overexpression in cultured human neuronal cells protects against hydrogen peroxide insult via activating phosphoinositide-3 kinase and opening the mitochondrial K(ATP) channel. *Antioxid Redox Signal*. 2010;13(6):769–781.
19. Raida Z, Hundahl CA, Nyengaard JR, Hay-Schmidt A. Neuroglobin over expressing mice: expression pattern and effect on brain ischemic infarct size. *PLoS One*. 2013;8(10):e76565.
20. Hundahl CA, Luuk H, Ilmjärvi S, et al. Neuroglobin-deficiency exacerbates Hif1A and c-FOS response, but does not affect neuronal survival during severe hypoxia in vivo. *PLoS One*. 2011;6(12):e28160.
21. Petit L, Ma S, Cheng SY, Gao G, Punzo C. Rod outer segment development influences AAV-mediated photoreceptor transduction after subretinal injection. *Hum Gene Ther*. 2017;28(6):464–481.
22. Umino Y, Solessio E, Barlow RB. Speed, spatial, and temporal tuning of rod and cone vision in mouse. *J Neurosci*. 2008;28(1):189–198.
23. Szél A, Röhlich P, Caffé AR, van Veen T. Distribution of cone photoreceptors in the mammalian retina. *Microsc Res Tech*. 1996;35(6):445–462.
24. Brittain T. The anti-apoptotic role of neuroglobin. *Cells*. 2012;1(4):1133–1155.
25. Guidolin D, Tortorella C, Marcoli M, Maura G, Agnati LF. Neuroglobin, a factor playing for nerve cell survival. *Int J Mol Sci*. 2016;17(11):1817.
26. Allore G, Petroustos D. Photoreceptor-dependent regulation of photoprotection. *Curr Opin Plant Biol*. 2017;37:102–108.
27. Han Z, Conley SM, Naash MI. Gene therapy for Stargardt disease associated with ABCA4 gene. *Adv Exp Med Biol*. 2014;801:719–724.
28. Ochakovski GA, Bartz-Schmidt KU, Fischer MD. Retinal gene therapy: surgical vector delivery in the translation to clinical trials. *Front Neurosci*. 2017;11:174.
29. Shintani K, Shechtman DL, Gurwood AS. Review and update: current treatment trends for patients with retinitis pigmentosa. *Optometry*. 2009;80(7):384–401.
30. Yu DY, Cringle SJ. Retinal degeneration and local oxygen metabolism. *Exp Eye Res*. 2005;80(6):745–751.
31. Nowak JZ. Oxidative stress, polyunsaturated fatty acids-derived oxidation products and bisretinoids as potential inducers of CNS diseases: focus on age-related macular degeneration. *Pharmacol Rep*. 2013;65(2):288–304.
32. Yu Z, Xu J, Liu N, et al. Mitochondrial distribution of neuroglobin and its response to oxygen-glucose deprivation in primary-cultured mouse cortical neurons. *Neuroscience*. 2012;218:235–242.
33. Raychaudhuri S, Skommer J, Henty K, Birch N, Brittain T. Neuroglobin protects nerve cells from apoptosis by inhibiting the intrinsic pathway of cell death. *Apoptosis*. 2010;15(4):401–411.
34. Meira LB, Moroski-Erkul CA, Green SL, et al. Aag-initiated base excision repair drives alkylation-induced retinal degeneration in mice. *Proc Natl Acad Sci U S A*. 2009;106(3):888–893.
35. Zulliger R, Lecaude S, Eigeldinger-Berthou S, Wolf-Schnurrbusch UE, Enzmann V. Caspase-3-independent photoreceptor degeneration by N-methyl-N-nitrosourea (MNU) induces morphological and functional changes in the mouse retina. *Graefes Arch Clin Exp Ophthalmol*. 2011;49(6):859–869.
36. Reisenhofer M, Balmer J, Zulliger R, Enzmann V. Multiple programmed cell death pathways are involved in N-methyl-N-nitrosourea-induced photoreceptor degeneration. *Graefes Arch Clin Exp Ophthalmol*. 2015;253(5):721–731.
37. Kuro M, Yoshizawa K, Uehara N, Miki H, Takahashi K, Tsubura A. Calpain inhibition restores basal autophagy and suppresses MNU-induced photoreceptor cell death in mice. *In Vivo*. 2011;25(4):617–623.
38. Yousefi S, Perozzo R, Schmid I, et al. Calpain-mediated cleavage of Atg5 switches autophagy to apoptosis. *Nat Cell Biol*. 2006;8(10):1124–1132.
39. Mizukoshi S, Nakazawa M, Sato K, Ozaki T, Metoki T, Ishiguro S. Activation of mitochondrial calpain and release of apoptosis-inducing factor from mitochondria in RCS rat retinal degeneration. *Exp Eye Res*. 2010;91(3):353–361.
40. Barabas P, Cutler Peck C, Krizaj D. Do calcium channel blockers rescue dying photoreceptors in the Pde6b (rd1) mouse? *Adv Exp Med Biol*. 2010;664:491–499.
41. Pasantes-Morales H, Quiroz H, Quesada O. Treatment with taurine, diltiazem, and vitamin E retards the progressive visual field reduction in retinitis pigmentosa: a 3-year follow-up study. *Metab Brain Dis*. 2002;17(3):183–197.
42. Chan AS, Saraswathy S, Rehak M, Ueki M, Rao NA. Neuroglobin protection in retinal ischemia. *Invest Ophthalmol Vis Sci*. 2012;53(2):704–711.
43. Fago A, Mathews AJ, Brittain T. A role for neuroglobin: resetting the trigger level for apoptosis in neuronal and retinal cells. *IUBMB Life*. 2008;60(6):398–401.

## Therapeutics and Clinical Risk Management

### Publish your work in this journal

Therapeutics and Clinical Risk Management is an international, peer-reviewed journal of clinical therapeutics and risk management, focusing on concise rapid reporting of clinical studies in all therapeutic areas, outcomes, safety, and programs for the effective, safe, and sustained use of medicines. This journal is indexed on PubMed Central, CAS,

Submit your manuscript here: <http://www.dovepress.com/therapeutics-and-clinical-risk-management-journal>

Dovepress

EMBASE, Scopus and the Elsevier Bibliographic databases. The manuscript management system is completely online and includes a very quick and fair peer-review system, which is all easy to use. Visit <http://www.dovepress.com/testimonials.php> to read real quotes from published authors.